DISCRETE STATES OF REDSHIFT AND GALAXY DYNAMICS III, ABNORMAL GALAXIES AND STARS

W. G. Tifft
Steward Observatory
University of Arizona
Tucson, Arizona

Received 1975 June 20

Revised 1976 March 11

ABSTRACT

The redshift pattern in M82 is shown to be consistent with the multiple redshift concept as are redshift differentials in other active objects. The presence of multiple redshift states and the general lack, therefore, of violent motion appears consistent with all types of galaxies.

Within our own Galaxy evidence is examined for effects of multiple redshift effects in stars. Four possibilities are considered; interstellar material, pre main sequence objects, rotation in massive stars, and highly evolved or peculiar stars. All classes show evidence of the predicted redshift periodicity. Stellar rotation in particular, is shown to occur preferentially in steps of 72.5 km s^{-1}. Implications of the correlations are briefly discussed.

INTRODUCTION

In the first two sections of this paper, (Tifft 1976a, b DSR1, DSR2), the concept of the redshift as a discrete variable has been developed for normal single galaxies, and for multiple galaxies and clusters. A model of single galaxies consisting of two opposed streams with an intrinsic difference of redshift of 70-75 km s^{-1}, or multiples thereof, was developed in DSR1. In DSR2 evidence was presented indicating that redshift differences between galaxies can occur only in multiples of the same basic interval. Using large redshift intervals the periodicity was found to be close to 72.5 km s^{-1}. In this paper we consider further classes of objects, active or abnormal galaxies, and stars within our own Galaxy. The former demonstrates the consistency of the discrete redshift model for extreme conditions. The latter provides evidence for multiple states within the Galaxy as required by the DSR1 model.

ACTIVE OBJECTS

Unusual activity in galaxies may range from the extreme concentrated nuclear activity of Seyfert galaxies to the more mild central "explosions" and disruption in galaxies such as M82. No completely satisfactory theories exist to explain the nuclear activity but it is generally considered that the objects represent various degrees or stages of a basic phenomenon which is probably closely related to activity in the QSS.

Figure 1 presents redshift data on the major axis of M82. Observations in position angle 57°-69° and out to 45" are shown, as observed by

Burbidge, Burbidge and Rubin (1964). Filled circles refer to emission line measurements and the large open circles to absorption line data. The absorption line material, including points at greater radii, is of low accuracy but defines a generally smooth rotation curve with a slope near 105 km s^{-1} arc-min^{-1} in the central regions. Figure 2a is the histogram of the redshift distribution, corrected for rotation using the absorption line slope, in the radius interval 10" to 45". It is apparent that the redshift distribution is not continuous. The power spectrum in Figure 2b shows a periodicity near 79 km s^{-1} quite consistent with the multiple redshift hypothesis.

After studying the M82 redshift patterns in various position angles from the discrete redshift viewpoint, it becomes apparent that the data can be fit by two principal redshifts, one near 285 km s^{-1}, dominant in the NE, and the other near 210 km s^{-1} dominant in the SW. Patches of a 140 km s^{-1} redshift also occur on the SW and a major cloud of 360 km s^{-1} material with some 430 km s^{-1} material occurs near the nucleus on the NE. It is this major cloud of 360 km s^{-1} material that turns the histogram in Figure 2 into a three peaked distribution. The strength of this cloud accounts for much of the "velocity" abnormality of M82. The region involved corresponds with the major dust lane that cuts through M82 NE of the nucleus.

In order to see the dominant role of the 285 km s^{-1} and 210 km s^{-1} redshift states, it is helpful to consider the redshift data taken at position angles away from the major axis. In Figure 3a the Burbidge, Burbidge and Rubin (1964) redshift data for position angle 0° is shown. The spectrogram was taken through the nucleus at about a 60° angle from the major axis. A small amount of rotation is therefore present. Beginning at the north end the data is well represented by the 285 km s^{-1} redshift

state. Near the nucleus, a rapid transition to the 210 km s^{-1} redshift state occurs. The 210 km s^{-1} state mixed with the 140 km s^{-1} state well represents the southern part of the spectrogram. The abnormally high redshift material is mostly to the east; it appears strongly at position angle 30^{o}. Figure 3b presents the Burbidge, Burbidge and Rubin (1964) redshift data for position angle 145^{o}. This spectrogram was nearly perpendicular to the major axis but passes several arc seconds west of the nucleus. In this case, the 210 km s^{-1} material is present on both sides of the nucleus with the 140 km s^{-1} state additions especially clear to the south. The 285 km s^{-1} state is limited to the northwest and a small amount of 360 km s^{-1} material is seen between 50" and 70" which is where the major dark lane, noted previously, cuts across the spectrogram. Since M82 is apparently seen nearly edge-on, the minor axis will show neither expansion nor rotation effects and the state lines are at constant redshift.

The multiple redshift concept appears completely able to accommodate the redshift pattern in M82 and requires or permits no high material velocities. The activity in M82 can perhaps be related to the presence of an abnormal amount of a third major redshift state. Great quantities of dust apparently accompany this condition. One is immediately reminded of other active objects like Centaurus A. Before leaving M82, it should also be noted that the redshifts quoted for the M82 states are galactocentric and are directly consistent with values in Figure 10 of DSR2. Thus M82 is consistent with the argument against large scale motion between galaxies in unrelated groups.

Most investigations of active galaxies, unlike the study of M82, involve spectroscopy of the nucleus only. A frequent result of such studies is that "high velocity" clouds of "ejected" material are seen. For redshift differentials up to about 500 km s^{-1}, there appears to be

good agreement with intervals expected from the multiple redshift concept. One of the most interesting cases is NGC 4151, a Seyfert galaxy, in which Anderson and Kraft (1969) detected narrow displaced absorption lines. HeI shows several displaced absorption components, the lowest one being at -280 km s^{-1} with respect to the main emission redshift. In another study, Walker and Hayes (1967) investigating emission in the nucleus of M87 concluded that a high velocity cloud was seen at -210 km s^{-1}.

Further indication of "high velocity" cloud motion has been inferred from line doubling. Sargent (1972) observed line doubling in Markarian 78, however, it is not possible from his notes to distinguish rotation from line splitting. Anderson (1973) shows that emission in the Seyfert galaxy NGC 7469 is double. Anderson (1973) also provided observations of the outer portions of NGC 7469 for rotation analysis. Very clear asymmetries of 70-75 km s^{-1} are present, making NGC 7469 another good candidate for dual redshift modeling. DuPuy (1970) has reported line structuring in several Haro galaxies, however, attempts by the author to verify these have so far been negative. Numerous examples of emission line and emission region doubling were given for components of double galaxies in DSR2. Finally we should add the observation of the doubling of certain QSS absorption lines at 141 km s^{-1} as noted by Boksenberg and Sargent (1975).

Table 1 summarizes data on line doubling and cloud "velocities". The first column gives the multiplicity, N, of the redshift state spacing required to account for the tabulated redshift differentials. All values to N=5 are readily accounted for by the multiple redshift concept. Too few higher values occur to evaluate any regularity. One difference between the mildly active double galaxies and the active Seyfert class of objects seems to be that some greater displacements are present in the

latter. Even the extremely broad hydrogen line profiles of type I Seyfert galaxies could possibly be constructed from a superimposition of many states seen simultaneously. This type of explanation may be particularly appropriate for the broad forbidden lines of type II Seyfert galaxies. The line splitting observed in many of the double galaxies previously discussed could easily be mistaken for broadened lines at lower dispersion, especially if widening is used. Widening would tend to blur together the slightly spatially separated components which seem to be characteristic of most of these galaxies. This is not to say that the lines are always intrinsically narrow. The lines in K 363B and K 93, another double line Seyfert type object, are certainly broadened as well as doubled. The broadening in these cases appears to be on the order of 100 km s^{-1} rather than many hundreds.

The displaced absorption line phenomenon seen in NGC 4151 and well known in absorption line QSS has certain characteristics. The displacement is almost always to negative redshifts and the lines are generally narrow. Scargle (1973) has discussed the production of such lines by the line-locking mechanism. There are severe problems of stabilizing and confining such clouds while they are accelerated to high velocity and it seems improbable that the medium so treated would remain as quiescent as the line widths indicate. Another argument against line locking is now possible. Specific observable cloud velocities are possible only in the line of sight, at other angles variable projection factors will enter. Thus emission line splitting from such clouds when laterally separated should be less than the absorption values and in general cannot have a discrete pattern. The data indicate no distinction between absorption and emission.

The time systematic sense of redshift evolution implied in the non-dynamical discrete redshift concept requires that if "transitions" occur, primarily lower redshift states will appear. If Seyfert nuclei represent a major transition phase, it is reasonable that new material would appear primarily at systematically negative redshifts as observed. The absence of violent motion is also consistent with the narrow line profiles, and projection effects do not enter. Line of sight absorption-line and laterally separated emission-line redshift differentials will be the same as observed.

In summary, there is no evidence among active objects that is inconsistent with the concepts set forth in this series of papers.

LOCAL EFFECTS OF MULTIPLE REDSHIFT STATES

From the discussion in DSR1, our Galaxy can be pictured as an ordered mixture of redshift states. The state present locally should be dominantly zero since this is by definition the state which our own material represents. The other primary state in our Galaxy is negative 70-75 km s^{-1}, however, to minimize speculation on any mechanisms of state production, we will rely mostly on the usual continuity and periodicity analysis rather than a prediction of specific states. The periodicity appears to be well determined from DSR2; the first six states away from zero are ±72, ±145, ±217, ±290, ±362 and ±435 km s^{-1}.

Two basic effects will be produced if there is some intermixing of states. First, there could be some direct effects in stellar kinematics. This effect is not likely to be very noticeable, however, since the sun seems to be located well within a single redshift stream. Occasional interlopers will most likely be lost in the normal velocity dispersion

of stars. Thus, local kinematics cannot obviously argue for or against the multiple redshift state hypothesis. A second effect in stars, however, could arise if small amounts of different states were intermixed upon formation of a star or produced in certain types of stars or during some stages of stellar evolution. In this case, direct spectral manifestations in the form of displaced, multiple, or broadened spectral lines could appear. Four cases will be examined here beginning with interstellar material and then considering stars in formation, massive early type stars, and advanced stages of evolution or other peculiar objects.

INTERSTELLAR MATERIAL

Some aspects of interstellar material in our Galaxy were considered in DSR1 where the general modeling of HI was discussed. Somewhat more locally, the pattern of "velocity" in the high velocity clouds was demonstrated to show a 70-75 km s^{-1} periodicity. In both of these cases, a general knowledge of the true rotational and expansion pattern in our Galaxy is required to see effects clearly. One further manifestation in HI which has recently appeared in the literature is of interest in the multiple redshift context. Simonson (1975) has discussed anomolous HI clouds in the anticenter region and interpreted them as due to a dwarf galaxy satellite of the Milky Way. The data show a cloud of material which parallels the velocity-longitude pattern of the Galaxy, but is displaced from it by 90 km s^{-1}. Except for the general slope of the pattern with longitude, the HI pattern near the anticenter is insensitive to a rotation model but will show full effects of any differential Galactic expansion. Any negative 70-75 km s^{-1} material in the anticenter at fairly large distances where the expansion effect may approach zero must appear

displaced from the local hydrogen by approximately -72-18 = -90 km s^{-1}. The second term is the solar expansion rate suggested in DSR1. Thus any distant -72 km s^{-1} material in the anticenter direction should appear precisely where the "satellite" appears. Its absence would be more unexpected than its presence in the multiple redshift concept. Similar reasoning can be used to predict that redshifts of components of the galactic nucleus can occur at n·72.5+18 km s^{-1} or -54, -127, -199, etc. as shown to be the case in DSR1.

One further aspect of interstellar material concerns gas which could produce optical interstellar lines. To avoid ambiguity with shifts due to galactic rotation and uncertain distances, the test can be applied unambiguously only to fairly local stars. The list of interstellar CaII velocities of Adams (1949) contains four stars with large negative displacements. Information on the four stars is given in Table 2. The mean displacement of this negative component with respect to the "local" material is -70 ±5 km s^{-1} (mean error of mean). There are several large positive deviations, one of +96 km s^{-1}, but there are too few stars to produce a clear pattern. The overall distribution of velocities is strongly concentrated near zero. The presence of an unexpectedly large number of large ΔV, considering the generally narrow distribution, is directly consistent with the multiple redshift concept as is the mean ΔV of the negative clump in Table 2. It is difficult to see how any significant numbers of clouds could maintain high real velocities in view of the efficiency of intercloud collisions for dissipation of kinetic energy. It is also difficult to devise methods of accelerating clouds. These problems vanish with the multiple redshift concept.

PRE MAIN SEQUENCE STARS

From both the previous brief discussion of interstellar material, and the observation that dust complexes often appear to be associated with redshift state boundaries, it is reasonable to look into dust-gas regions for multiple redshift effects. It is in such regions that pre main sequence stars are seen in the form of Herbig-Haro objects and T Tauri stars. These types of objects are therefore prime candidates to show multiple redshift phenomena. In the process of gravitational collapse in a cloud where one state of matter is dominant, it is reasonable to assume that various quantities of other states would be swept along. As formation progresses, clouds or bubbles of incompatible states could be rejected and result in a haze of material which would produce emission or absorption features with various displacements from the actual center of mass motion of the dominant state material. A natural mechanism for the instability observed in pre main sequence stars would exist and certain patterns should be present in line profiles. It is not likely that entrapped material could attain especially high real velocity very near a star due to the very effective resistance of the dominant material in which it is presumably embedded. Thus to first order displaced line components should appear close to standard state spacings of 72.5 km s^{-1} or multiples thereof. Since some real motion will certainly be present there will be blurring, especially near the dominant state. The higher multiples of the state spacing when present should be the most clearly seen and the larger displacements should presumably conform best to predicted state values.

A high dispersion study of several T Tauri stars was carried out by Kuhi (1964). Profiles of various emission lines in various stars were reproduced in his paper and several representative ones have been transcribed for reproduction in Figure 4. Examination of these profiles shows that characteristic humps or dips appear at the spacing expected from multiple states. The profiles could be readily constructed as a summation over a series of independent lines at the standard state spacing. No intermediate states would be required. Note especially how well the small negative peak in T Tauri and the triple nature of the positive RY Tauri peak fit the predicted pattern. The case of Lick Hα-120 is especially interesting. The strong negative absorption feature corresponds very closely to a -290 km s^{-1} component. A corresponding +290 km s^{-1} emission feature appears to be present in the K line. Several other stars presented by Kuhi (1964) fit the multiple profile pattern equally well.

Two other T Tauri stars with clear negative absorption "shell" components have been discussed by Herbig (1966, 1973). FU Orionis shows a "shell" absorption spectrum displaced -80 km s^{-1} from the underlying star. BD-10°4662 is a double T Tauri object both components of which show Hα emission displaced -55 to -82 km s^{-1}. Both cases are clearly compatible with -72 km s^{-1} material rather than motion. Strom, Grasdelen, and Strom (1974) have made a study of Herbig-Haro objects. In general the objects show negative "velocities" with respect to the clouds with which they are associated. The two most extreme cases are HH-11 at -146 km s^{-1} and HH-100 at -141 km s^{-1}. Line profiles are not given, and since the dispersion used would barely resolve 70 km s^{-1}, it is not possible to determine if the lines can be constructed of superimposed state profiles.

On the basis of the limited material available, especially at high dispersion, the pre main sequence stars appear quite compatible with the presence of multiple states. The expected preference for negative states is clearly present. No mechanism for massive ejection at the observed "velocities" is known. Much further high dispersion work on line profiles of pre main sequence objects will be required to test the hypothesis that multiple matter states are responsible for the "velocity" patterns found. It is certainly interesting, but obviously not definitive, that no exceptions to the multiple state pattern are present in the studies known to the author.

EARLY TYPE STARS AND STELLAR ROTATION

In the two previous sections, interstellar lines and pre main sequence stars, one is perhaps seeing multiple states because the two stream model for galaxies predicts that they already exist in the interstellar material. The statistics are obviously limited and perhaps the most one can say is that the data are not inconsistent with the multiple redshift concept. Further tests are clearly needed. A second approach to tests of the multiple state hypothesis in stars is less obvious but especially interesting from the viewpoint of understanding the process of state production. If one draws an analogy between conventional atomic fusion and possible matter state transitions, it follows that the higher the temperature and pressure to which matter is subjected, the more likely one is to eventually reach a point where transitions occur. Without making any claims about the physics of such transitions, if they indeed exist, there is no reason to rule out a possibility of seeing effects. Stars hotter than the sun are obviously required since the sun shows no obvious spectral peculiarities which fit the multiple redshift concepts.

If state transitions can occur in cores of certain stars, then possible non-normal gravitational interactions between states hypothesized in DSR2 provide a mechanism for the diffusion of the material away from the core. The energy and pressure balance conditions in the core will be modified to various degrees depending upon the amount of production involved. Material arriving in the outer layers of the star will produce displaced line components. Depending upon the natural widths and strengths of the lines, the components may be distinguished or the line

may be simply broadened. If states were produced asymmetrically with respect to the dominant state, a change in the systemic measured "velocity" of the star should occur. One can therefore immediately rule out a strongly asymmetric effect since no gross K effects are observed in studies of early type stars. Small systematic "velocity" effects and unexplained variations in "velocity" remain as candidates for non symmetrical state mixtures. For state production in a symmetrical fashion, the principal effect will be to broaden spectral lines. The effect should therefore be intermingled with effects of stellar rotation. This is an interesting possibility in view of some of the unexplained phenomena in the interpretation of stellar rotation data.

Figure 5 illustrates the effect of line blending for components with differing ratios of width to separations. Simple Gaussian profiles were used. It is apparent that separate components will not appear in a line until the 1σ spread of the individual components drops to nearly 1/3 of the component separation. It therefore follows that for natural 1σ spreads of 30 km s^{-1} or larger, a single smooth profile would be observed for lines formed from multiple states. The critical distinction between rotation and multiple states formed in symmetrical pairs and blended together is that rotation is a continuous variable while multiple states will produce "steps" in line widths. The test for multiple states is therefore to look for a 72.5 km s^{-1} periodicity in published rotational "velocities". A preliminary survey of B star rotation was carried out using the complete sample of B stars tabulated by Uesugi and Fukuda (1970). Stars were counted in bins of 1/2 state width centered on and midway between states, i.e. 0-18, 19-55, 56-91 km s^{-1}, etc. If a state periodicity is present, the on-state bins should be enhanced and the off-state bins

depressed. The distribution should be smooth within statistical fluctuations for rotation. The result appears in the upper-most panel of Figure 6 while the counted numbers are summarized in Table 3. The figure shows a clear sawtooth pattern with enhanced on-state bins.

Further interesting effects are brought out by separation of the B star sample by luminosity class. The two middle panels of Figure 6 show B0-B5 stars of luminosity class IV-V and I-III. These figures illustrate the previously known effect (Van den Heuvel 1968) that B-F stars contain distinct slow and fast "rotational" groups. Beta Canis Majoris stars concentrate in the slow rotational B star group. The interesting point of the figure is that the break occurs right at the first state value. Giant stars, on the other hand, peak precisely at this value. The location of steps in the total distribution and the match of the rotational break with the first state value are remarkable coincidences if accidental.

The final panel of Figure 6 illustrates the distribution of rotation for B emission and shell stars as tabulated by Bernacca and Perinotto (1971). The interesting point here is that the final break or upper limit again occurs at a predicted state value. In general, therefore, the survey of a large B star sample gives positive support to the hypothesis that B star line widths occur preferentially in multiples of 72.5 km s^{-1}. This does not mean, of course, that real rotation does not enter or can even be large in certain cases. It does, however, suggest that rotation alone is not the broadening mechanism.

The material in Figure 6 includes a wide range in quality and is derived from many separate sources, hence is not suitable for statistical analysis. As with the periodicity analysis of the Coma cluster redshifts in DSR2, any effect seen should strengthen as higher quality data are

considered. B star data were therefore compiled separately for the most recent studies at highest spectral resolution. References in the Uesugi and Fukuda (1970) catalog with the highest weight were utilized as well as more recent work. For inclusion most measures had to be obtained from spectrograms with dispersions of 30 A mm^{-1} or less. Field stars and cluster stars were separated to give independent samples. Tables 4 and 5 contain the data, including the references. The results are shown in Figure 7. It is seen that the steps in the general distribution have now become distinct peaks and valleys.

The third panel of Figure 7 gives the sum of the cluster and field star distributions. This total best B star sample will now be considered for significance testing. The low end of the distribution is seriously distorted by limited spectral resolution which sets in between 10 and 40 km s^{-1} for the studies utilized. The first two bins will therefore not be considered further. The highest values of Vsini are also relatively uncertain because of the great difficulty in accurately measuring a very wide shallow profile. It is not surprising, therefore, that the periodicity shows best in the midrange. Despite the lower weight of the larger values, we shall include them in the significance calculations. From Figure 6a and the smoothed forms of Figure 7, it is apparent that the frequency distribution rises systematically toward zero. We wish to evaluate the significance of the periodic fluctuations from the smoothed function. If we begin at the high end of the distribution and form cumulative sums of on-state and off-state numbers, the innermost sum should be the largest for a smooth distribution. Consider the last three sums prior to reaching the resolution limit, these are the on-state sums in to the 72 and 145 km s^{-1} bins and the off-state sum in to the 108 km s^{-1}

bin. Call these sums S_{72}, S_{108}, and S_{145}. The smooth or rotational model requires that $S_{72}>S_{108}>S_{145}$. In fact we observe $S_{72}>>S_{108}<S_{145}$; the actual sums are given in Table 6. A simple χ^2 test comparing S_{108} with S_{145} for a hypothesis of equality will underestimate the significance of the state periodicity. Likewise, an equality comparison of S_{72} and S_{108} will overestimate the significance. Table 6 gives the probability limits just defined. The total sample is highly significant even at its lower limit. A conservative estimate for the overall preference of Vsini measuremnts to fall at state values is $p\simeq0.001$. The periodicity is highly significant by any standard. It is perhaps worth emphasizing here that the periodicity tested is not a free variable. The periodicity is predicted from previous considerations. There is no search for periodicities at unspecified frequencies.

Several studies were omitted from the data in the previous analysis. Most of these were studies at lower dispersion or older relatively imprecise ones. Two studies, which will be further considered now, tabulated Vsini only to the nearest 10 km s^{-1}. Such coarse steps can in principle lead to a significant decimal equation binning which could distort the statistics. The material in the above analysis was in general given to the nearest 5 km s^{-1}. At this level the decimal equation effects are relatively small compared to the fluctuations detected, especially in view of the level of significance found. In addition to giving accurate measurements of Vsini for selected O5-B2 stars, Slettebak (1956) provided estimates to the nearest 10 km s^{-1} for a sizeable additional number of stars. These data were transformed from listed turbulent "velocities" to Vsini using the calibrated sample and are shown in Figure 8 and Table 7. The high weight sample is shown for comparison from Table 4. The samples are

clearly indistinguishable. A second study by Slettebak (1968), in the Scorpio-Centaurus region, was also given only to 10 km s^{-1}. The third panel of Figure 8 contains this data. The correlation is weak but present.

The fifth panel in Figure 8 is a summation over three clusters studied by Levato (1974a, b, 1975). These studies were omitted from the precision study discussed above since they were all carried out at dispersions near 40 A mm^{-1}. They are included here for completeness and clearly show the same effects and can only add to the significance of the periodicity. Between Figures 7 and 8, virtually all the best B star investigations have been collected. There are no exceptions to the on-state enhancement pattern.

One final point is of interest in Figure 8. Three field samples and three cluster samples are shown. There appears to be a slight systematic difference in that the field stars concentrate more to lower states. The clusters tend to show an enhanced 217 km s^{-1} population. No attempt has been made to estimate its significance but if real, it would presumably be an age effect, the cluster stars on the average being younger than the field.

As soon as one considers stars later than B, the higher state population drops rapidly and a strong concentration appears near zero. To examine the A stars in some detail, studies by Abt, Chaffee, and Suffolk (1972) and Abt and Moyd (1973) will be considered. Both utilized spectroscopy at 13 A mm^{-1} or better to permit resolution near zero. The results are listed in Table 7 and illustrated in Figure 9. The well known effect that Am and Ap stars clump near zero while normal main sequence A stars avoid zero is well shown. What is particularly interesting, however, is that the break between the groups corresponds perfectly with the first

state boundary. The small fluctuations in the A star bin populations fit the state pattern adequately. Clearly the A stars do not detract at all from the multiple state hypothesis.

Beyond the A stars, rotational line widening drops dramatically so by the time one reaches G stars, no broad line stars remain. Table 8 and Figure 10 contains information on clusters and field stars which fall primarily in the F star range. The upper panel of Figure 10 shows clearly how the peak near zero is dominant, however, a distinct 72 and 145 km s^{-1} enhancement remains. The most precise study in this spectral range appears to be the Oke and Greenstein (1954) study of field stars, mostly luminosity class III, shown in the center panel of Figure 10. Oke and Greenstein (1954) noted that six bright standard stars omitted from their list were broad line stars which would fall in the 75-150 km s^{-1} interval. Thus the 72 and 145 km s^{-1} peaks shown may very well be underestimates.

The interpretation of broad lines in early type stars as due primarily to rotation has led to some intriguing problems. The existence of distinct slow and fast "rotational" subsets at the same spectral class, and the dramatic drop of "rotation" in the F stars being the most significant. Various mechanisms of rotational braking have been considered, including magnetic coupling with the surrounding medium. Distinct problems exist with all mechanisms. To this set of problems, the author now adds the periodicity in Vsini at 72.5 km s^{-1}. This complication is perhaps the key to the entire rotational dilemma. If the broad lines are due to multiple states of matter and not rotation, the braking problem vanishes. The onset of matter transitions with temperature is presumably a high power of the temperature as is the case in virtually all nuclear reactions. The sudden onset of line broadening in the F stars is therefore quite

logical. It must be emphasized again, however, that this mechanism does not necessarily rule out real rotational effects. There are, for example, rotational effects observed in eclipsing binaries which may still require a rotational interpretation. The entire question of binary stars is a separate question from the multiple state of matter viewpoint, however, and does not form a part of this paper.

ADVANCED STAGES IN STARS, PECULIAR STARS

The final line of evidence for manifestations of discrete "velocity" states in our galaxy concerns various special or peculiar stars which generally represent special or peculiar stages in stellar evolution. If stars can transform matter under certain conditions, as suggested in the last section, then such peculiar stars are a logical place to look. Stars showing effects which may be interpretable in the discrete states of matter concept do exist and have been recently discussed by Scargle (1973) with reference to line locking. Table 9 contains a summary of displaced components in five stars where the basic systemic velocity is adequately known to form a reliable differential.

The first three stars in Table 5 apparently give stable values of the differentials and except for two values in HD 190073, a better agreement with the multiple redshift differential pattern would be difficult to find. In the line locking and harmonic pairing discussed by Scargle, the -181 km s^{-1} line in HD 190073 is utilized and only the -323 km s^{-1} line is considered an "interloper". The absence of the -181 km s^{-1} line in XX Oph and υSgr is not explained. In the present scheme both the -181 and -323 km s^{-1} lines in HD 190073 are interlopers. The interesting thing

now, however, is that the difference between them is 142 km s^{-1}. Thus HD 190073 shows two systems with appropriate state spacings, one which can be considered to be essentially at rest and the other in a moving shell. All features are consistent.

The line structure in AG Peg is complex and quite rapidly variable. Scargle (1973), whose values for redshift are given in the table, has combined the components in a different manner than Merrill (1951) in his original tabulation. In this case real motion is sufficient to raise ambiguities as to proper identification, however, it is clear that the same range of displacement is present and by "proper" assignment of each component, the multiple redshift pattern is an acceptable fit.

All the stars in Table 5 are unusual in some regard. XX Oph is an R Coronae type variable, HD 190073 is an Ap shell star and AG Peg is a symbiotic nova like object. They are all stars for which it is quite reasonable to imagine that the internal structure has reached critical stages in evolution. It seems possible that under extreme conditions in such stars, detectable amounts of matter could be transformed between redshift states as already indicated for normal stars. The remarkable 1925 changes in XX Oph described by Merrill (1932) may be well described by the appearance, at the surface, of a "bubble" of -210 and -280 km s^{-1} redshift material. Other spectral peculiarity puzzles may find interesting possibilities in the multiple states of matter concept.

As a final example of stars where multiple matter states may play an important role, we shall consider novae. Novae are well known to show multiple "velocity" systems. One excellent example is nova Hercules of 1934 (McLaughlin, 1954) for which a very large number of measurements of displaced absorption components is available. There is no doubt that real

velocities are involved in novae, however, various differential "velocities" between what has been interpreted as multiple shells are subject to alternative modeling, at least in the earlier phases of development before more complex motion patterns build up.

The pattern presented by nova Hercules was as follows. From about 20 December 1934 until about 1 January 1935, when it disappeared, the premaximum (absorption I) system presented a stable velocity near -175 km s^{-1}. Beginning about 24 December 1934 the principal (absorption II) system appeared and remained very steady at -320 km s^{-1} through the entire month of January. During the first half of February, the "velocity" of system II underwent a distinct increase then leveled off and remained fairly steady again throughout March, near -390 km s^{-1}. Beginning very late in December, various members of higher "velocity" systems known as the diffuse enhanced (absorption III) systems appeared and within blending limitations also maintained very steady "velocities". Beginning with the transition in the "velocity" of system II in February, the pattern of displaced components became much more chaotic, although a good degree of ordered pattern returned in March.

The conventional picture of the nova requires successive ejection of shells at various velocities, with collisions between shells perhaps playing a part in accelerating the principal shell. Certainly after the transition in early February, real differential velocity effects can probably not be ignored. At the earlier stages, if one hypothesizes a single shell with multiple matter states moving in unison, the apparent "velocities" must show the periodic pattern of 72.5 km s^{-1}. Figure 11 presents the complete "velocity" pattern for systems I-III through January 31, 1935. Lines are drawn at various multiples of the standard state spacing using

system I as a base. It is apparent that systems I and II differ by precisely two states while system III is also well fit by higher multiples. A power spectrum analysis of system III "velocities" alone confirms the presence of the state periodicity at the 0.01 to 0.001 significance level. Figure 12 is the phase-frequency diagram produced by dividing each "velocity" by 72.46 and counting the number in each phase interval. The clear periodic nature of system III and the perfect phasing of all three systems is obvious. The multiple states of matter hypothesis clearly provides an excellent fit to the early stages of nova Hercules and eliminates the necessity of generating extremely high velocity secondary shells. Further investigations in novae are obviously required.

OVERVIEW

In the series of papers which this paper completes, the concept that the redshift can occur in discrete steps has been explored. The evidence rests on a series of periodicity tests which consistently show the presence of a basic periodicity of 72.5 km s^{-1} or its higher multiples. The strongest cases to which formal probability testing have been applied are 1) Internal patterns in M31, 2) Redshift periodicities in the Coma cluster 3) B star rotation and nova Hercules as discussed in this paper. In addition, many other data samples have been shown to be consistent while none are inconsistent. Many further tests and refinements are possible.

The immediate implications of the presence of the discrete pattern are 1) distinct limitations on real motion and 2) the necessity to give properties to matter such that the multiple redshift can arise, i.e.

REFERENCES

Abt, H. A. and Chaffee, F. H. 1957, Ap.J. 148, 459.

Abt, H. A., Chaffee, F. H., and Suffolk, G. 1972, Ap.J. 175, 779.

Abt, H. A. and Hunter, J. H. 1962, Ap.J. 136, 381.

Abt, H. A. and Moyd, K. I. 1973, Ap.J. 182, 809.

Adams, W. S. 1949, Ap.J. 109, 354.

Anderson, K. S. 1973, Ap.J. 182, 369.

Anderson, K. S. and Kraft, R. P. 1969, Ap.J. 158, 859.

Bernacca, P. L. and Perinotto, M. 1971, Contr. Obs. Astrophys. Univ. Padova in Asiago No. 250.

Boksenberg, A. and Sargent, W. L. W. 1975, Ap.J. 198, 31.

Burbidge, E. M., Burbidge, G. R., and Rubin, V. C. 1964, Ap. J. 140, 942.

DuPuy, D. L. 1970, A.J. 75, 1143.

Herbig, G. H. 1973, Ap.J. 182, 129.

Kraft, R. P. 1965, Ap.J. 142, 681.

Kraft, R. P. 1967, Ap.J. 148, 129.

Kuhi, L. V. 1964, Ap.J. 140, 1409.

Levato, H. 1974a, PASP 86, 940.

Levato, H. 1974b, A.J. 79, 1269.

Levato, H. 1975, Ap.J. 195, 825.

Merrill, P. W. 1932, Ap.J. 75, 133.

Merrill, P. W. 1951, Ap.J. 114, 338.

McGee, J. D., Khogoli, A., Baum, W. A., and Kraft, R. P. 1967, M.N. 137, 303.

McLaughlin, D. B. 1954, Ap.J. 119, 124.

McNamara, D. H. and Larsson, H. J. 1962, Ap.J. 135, 384.

McNamara, D. H. 1963, Ap.J. 137, 316.

Oke, J. B. and Greenstein, J. C. 1954, Ap.J. 120, 384.

Scargle, J. D. 1973, Ap.J. 179, 705.

Simonson III, S. C. 1975, Ap.J. (Letters) 201, L103.

Slettebak, A. 1954, Ap.J. 119, 146.

Slettebak, A. 1956, Ap.J. 124, 173.

Slettebak, A. 1968, Ap.J. 151, 1043.

Slettebak, A. and Howard, R. F. 1955, Ap.J. 121, 102.

Strom, S. E., Grasdalen, G. L and Strom, K. M. 1974, Ap.J. 191, 111.

Tifft, W. G. 1976, Ap.J. (15 May in press) DSR1.

Tifft, W. G. 1976, Ap.J. (submitted) DSR2.

Treanor, Fr. P. J. 1960, M.N. 121, 503.

Uesugi, A. and Fukuda, I. 1970, Contr. Inst. Astrophys and Kawasan Obs. Univ. of Kyoto No. 189.

Van den Heuvel, E.P.J. 1968, B.A.N. 19, 309.

Walker, M. F. and Hayes, S. 1967, Ap.J. 149, 481.

Mailing address:

William G. Tifft
Steward Observatory
University of Arizona
Tucson, Arizona 85721

TABLE 1

Differential Redshifts <500 km s^{-1} in Double and Active Systems

	Double Galaxies							Active Galaxies		
N	K83	K144	K181	K252	K288	K363	K466	M87	N4151	QSS
0			15							
1				65						
2										141
3					207			-210		
4	294	297		277			288		-280	
5						365				

TABLE 2

Stars With Large Negative ΔV Interstellar Lines

HD	m	sp	l_I	b_I	V(neg)	V(local)	ΔV
1976	5.4	B4	87	-10	-62.5	-2.0	-60.5
175754	7.0	B0p	344	-11	-77.0	+4.4	-81.4
190429AB	7.2/7.8	05/0	40	2	-59.0	+6.5	-65.5
212978	6.1	B3	63	-15	-74.5	-0.9	-73.6
						mean	-70.3 ± 4.6

TABLE 3

B stars by "Rotational" Groups

state	"V sin i"	B0-B9.5 (all)	B0-B5 (IV-V)	B0-B5 (I-III)	Be, B shell
0	0- 18	80	35	6	
	19- 54	162	57	26	3
1	55- 91	169	32	57	6
	92-127	136	50	15	7
2	128-163	139	61	14	14
	164-199	113	44	6	12
3	200-236	116	45		21
	237-272	78	23	8	30
4	273-308	73	31	3	27
	309-344	35	21		24
5	345-380	34	9	1	28
	381-417	11	4		11
6	418-453	4	2	1	1
	454-489	1	1		
7	490-526				2

TABLE 4

Highest Quality B Star Data (Field)

state	"V sin i"	(1) O5-B2	(2) B2-B5	(3) B8-B9.5	Field
0	0- 18	4	21	7	32
	19- 54	1	24	1	26
1	55- 91	12	19	13	44
	92-127	10	10	4	24
2	128-163	11	23	9	43
	164-199	4	15	4	23
3	200-236	1	18	6	25
	237-272	1	10	1	12
4	273-308	2	11	2	15
	309-344		14		14
5	345-380	1	6	2	9
	381-417		3		3
6	418-453		1		1

(1) Slettebak (1956) tracings from 10 A mm^{-1} spectra.
(2) Slettebak and Howard (1955) 30 A mm^{-1} spectra.
(3) Slettebak (1954) 30 A mm^{-1} spectra.

TABLE 5

Highest Quality B Star Data (Clusters)

state	"V sin i"	(1) I Lac	(2) α Per	(1) Pleiades	(3) I Ori	(4) IC4665	Clusters	Clusters + Field
0	0- 18		5		11	1	17	49
	19- 54	6	12	4	22	5	49	75
1	55- 91	4	14	1	6	6	31	75
	92-127	5	5	1	7	1	19	43
2	128-163	4	9	3	15		31	74
	164-199	1	4	2	10	1	18	41
3	200-236	2	13	5	11	6	37	62
	237-272	1	3	1	6	4	15	27
4	273-308		4	4	6		14	29
	309-344	1	2	1	1		5	19
5	345-380	2	2	1	1	1	7	16
	381-417		2				2	5
6	418-453				1		1	2

(1) Abt and Hunter (1962) 18 A mm^{-1} spectra.
(2) Abt and Hunter (1962), and Kraft (1967) both 18 A mm^{-1}. 4 common stars averaged.
(3) McNamara and Larsson (1962), McNamara (1963), and Abt and Hunter (1962) dispersions 10-20 A mm^{-1}. Common stars averaged.
(4) Abt and Chaffee (1967) dispersions 13-40 A mm^{-1}.

TABLE 6

Significance of State Periodicity in B Star "Rotation"

	S_{72}	S_{108}	S_{145}	p <	p >
Field Stars	137	76	93	. 19	.00003
Cluster Stars	121	59	90	. 01	.00001
Total Sample	258	135	183	.007	<.00001

TABLE 7

A Stars By "Rotational" Groups.

state	"V sin i"	A5-A8V	Am	Ap
0	0- 18		23	19
	19- 36	3	14	31
	37- 54	2	8	11
1	55- 91	26	10	10
	92-127	23	6	1
2	128-163	29	1	
	164-199	21		
3	200-236	12		
	237-272	9		
4	273-308	1		

TABLE 8

F Stars By "Rotational" Groups.

state	"V sin i"	(1) Praesepe	(2) A7-G0	(3) Hayades	(3) Coma	Total
0	0- 18	7	11	28	14	60
	19- 36	11	3	9	5	28
	37- 54	2	1	5	2	10
1	55- 91	9	4	6	3	22
	92-127	8	1	1	1	11
2	128-163	10	2	2	1	15
	164-199	4	1		3	8
3	200-236	3			1	4

(1) McGee, Khogali, Baum, and Kraft (1967) "adopted" values, mostly high dispersion.

(2) Oke and Greenstein (1954) 2-10 A mm^{-1} spectra, omits stars later than G0.

(3) Kraft (1965) 5-20 A mm^{-1}. Values from Treanor (1960) omitted.

TABLE 9

Displaced Absorption in Stars

N	XX Oph	υ Sgr	HD 190073	AG Peg	V1057 Cyg
1	- 72			- 72	- 80, - 78
2	-144	-153	-147	-110, -154	
3	-203	(-202)	-200	-183, -229	
4	-296	-299	-296	-288	-282
5	-366		-358	-334, -382	-343
6			(-396)	(-428)	
?			-181		-180, -181
?			-323		

others +34, -28

FIGURE CAPTIONS

Figure 1 The major axis redshift pattern in M82 adapted from Burbidge, Burbidge and Rubin (1964). The large open circles refer to absorption line measurements which define the basic rotation curve. Five redshift states are suggested with the two which appear to be dominant in the galaxy shown connected. The strong positive redshift excess to the northeast may be abnormal.

Figure 2 The left (a) diagram is a histogram of the redshift data 10"<R<45" on the major axis of M82 after correction for rotation. The triple peaked distribution has the power spectrum shown in the right (b) diagram.

Figure 3 Redshift patterns in M82 at large angles to the major axis, adapted from Burbidge, Burbidge and Rubin (1964). The upper (a) panel is based upon a 0^{o} position angle spectrogram which makes an angle of $\simeq 60^{o}$ with the major axis. The lower (b) panel is based upon a 145^{o} position angle spectrogram which passes west of the nucleus and is nearly perpendicular to the major axis. Both spectrograms can be interpreted in terms of the presence of two basic and two secondary redshift states as shown.

Figure 4 T Tauri star line profiles adapted from Kuhi (1964). Intensity is in units of the continuum = 1. T Tau and RY Tau are shown with marks at state spacings with respect to a central velocity indicated. The profiles show

emission humps at each position suggesting a compound profile. Lick Hα-120 shows absorption dips as well as emission, again with state spacings as indicated. The location of CaII K line features is indicated with a K. An especially prominent emission peak occurs near +300 km s^{-1}.

Figure 5 The effect of overlapping equal Gaussian profiles at 1, 2, or 3 sigma. The sum will appear as a broadened feature rather than multiple until the profiles are separated by nearly 3σ. If the profiles are spaced at the 72.5 km s^{-1} state spacing, the individual profile sigma's correspond to 72, 36, and 24 km s^{-1}. It follows that for objects with natural line dispersions of 30 or more km s^{-1} the blending of several states will produce a single broadened line.

Figure 6 The distribution of B star rotational "velocities" from the Uesugi and Fukuda (1970) catalog or, for Be and B shell stars, from Bernacca and Perinotto (1971). For the latter the dashed line indicates data with p.c.<20 km s^{-1}. The numbers were counted in bins centered on or between state values. The breaks in the distribution invariably correspond to multiples of the basic 72.5 km s^{-1} state spacing.

Figure 7 The distribution of B star rotational "velocities" for the highest accuracy observations. The numbers were counted in bins the same as figure 6. Field stars, cluster stars, and the combination are shown. A $\sqrt{N}$ error bar is shown by the vertical lines. The accurate

data converts the steps in figure 6 into an obvious periodicity.

Figure 8 The distribution of B star rotational "velocities" for three slightly lower weight samples shown with the best samples for comparison. The basic 72.5 km s^{-1} periodicity pervades all the samples.

Figure 9 The distribution of A star rotational "velocities" from the most accurate material available. The location of the break between the peculiar and normal A stars corresponds to the first state boundary.

Figure 10 The distribution of late A and F star rotational "velocities" from the most accurate material available. Most "rapid rotators" have disappeared, however, the characteristic clumping of state values of 72 and 145 still persists.

Figure 11 Absorption line "velocities" in Nova Hercules 1934 from McLaughlin (1954). Lines at standard state spacings with respect to the premaximum absorption system I are shown. Beginning in late January the primary system II shifted rapidly to the next level as shown by arrows. In general, the state lines well represent the data allowing for occasional blending; lines specifically indicated as blended by McLaughlin are omitted. K line and Hα "velocities" are shown with crosses.

Figure 12 The phase (decimal part of V/72.5) distribution for all Nova Hercules 1934 "velocities" shown in figure 11. The periodicity and common phasing of the absorption systems is easily seen.

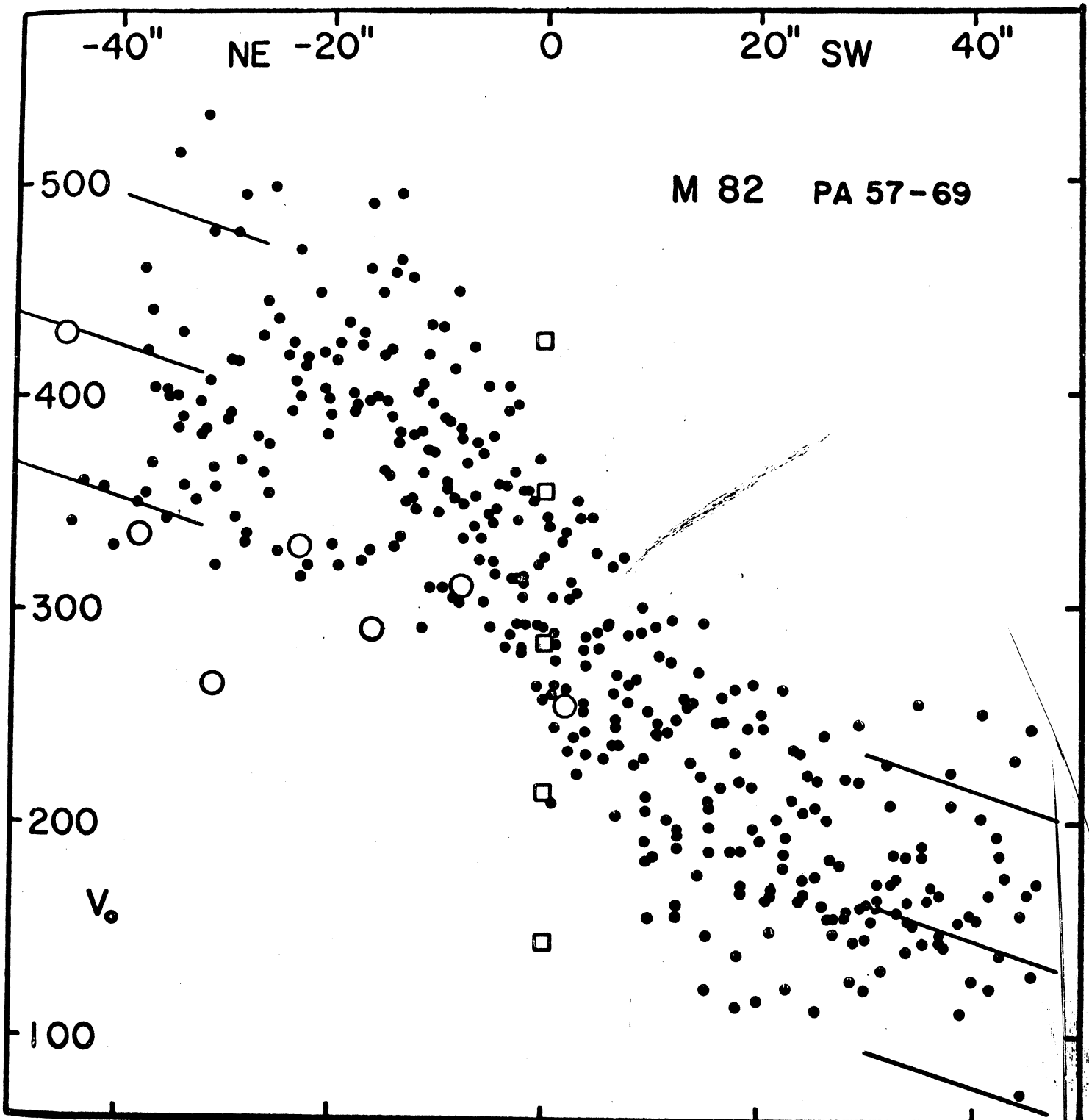
-40"
NE
-20"
0
20"
SW
40"
500
400
300
200
100
V_o
M 82 PA 57-69

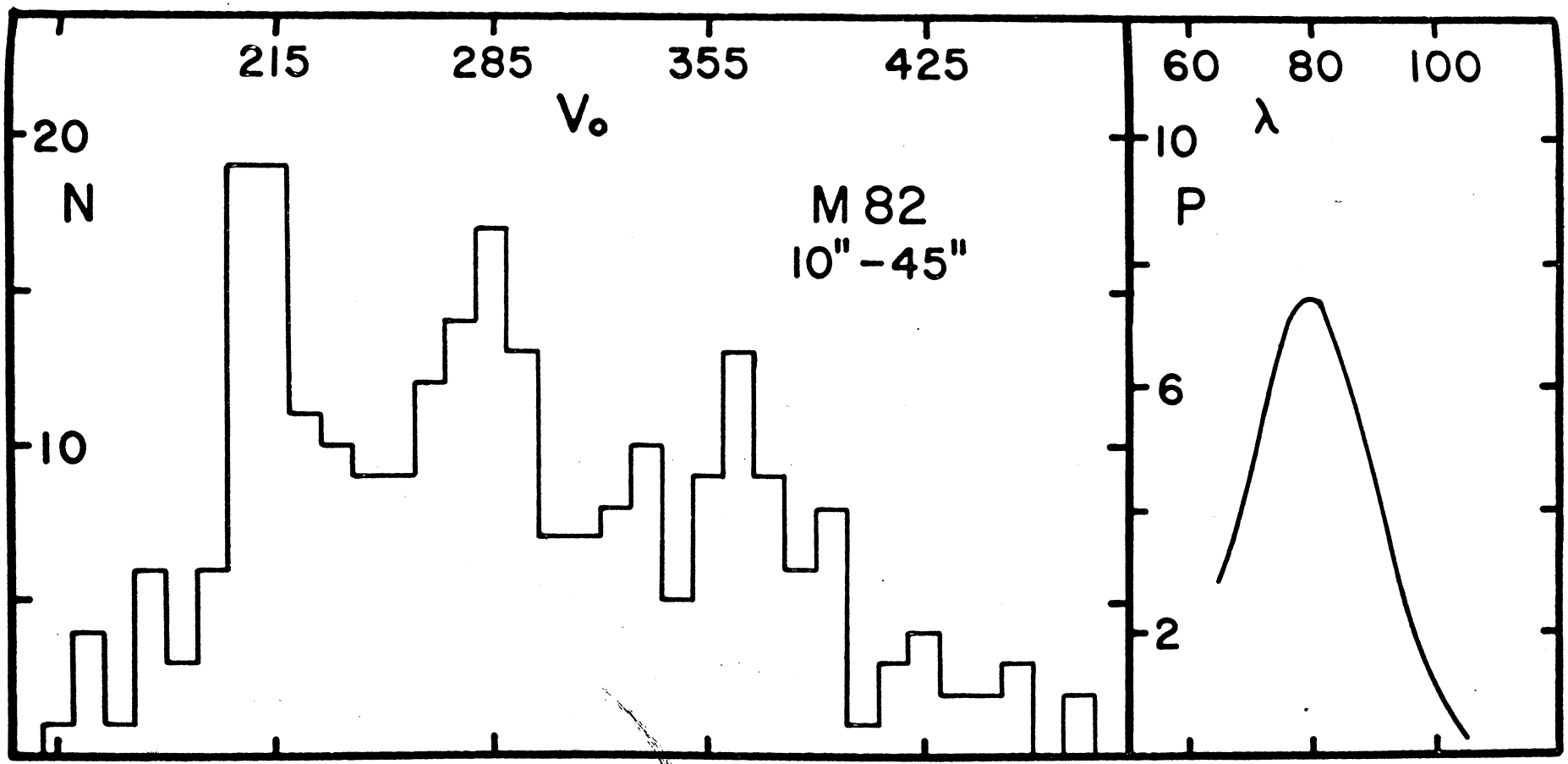
215
285
355
425
V_o
20
N
10
M 82
10"-45"
60
80
100
λ
10
P
6
2

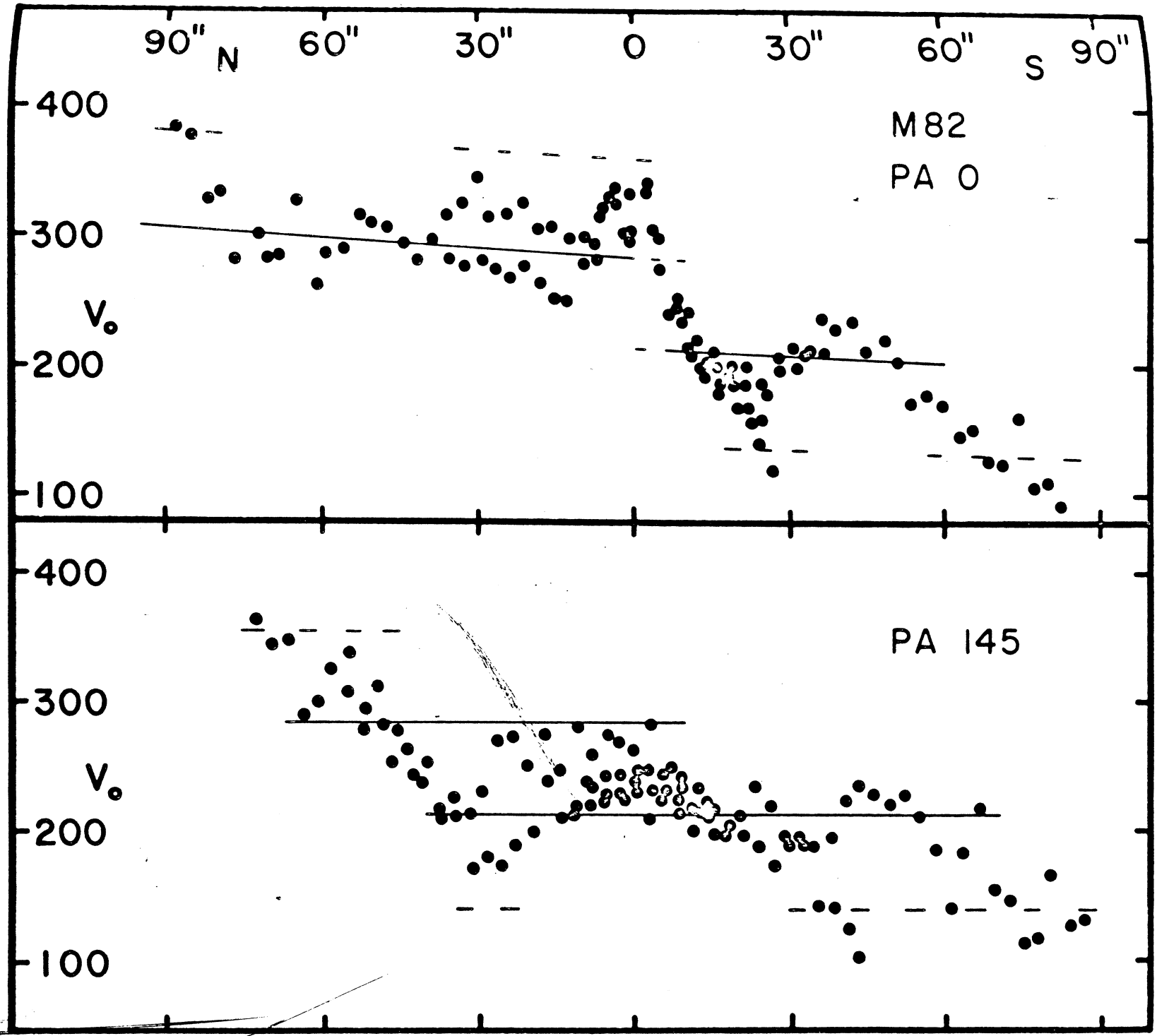
90" N
60"
30"
0
30"
60"
S 90"
400
300
200
100
V_o
M82
PA 0
400
300
200
100
V_o
PA 145

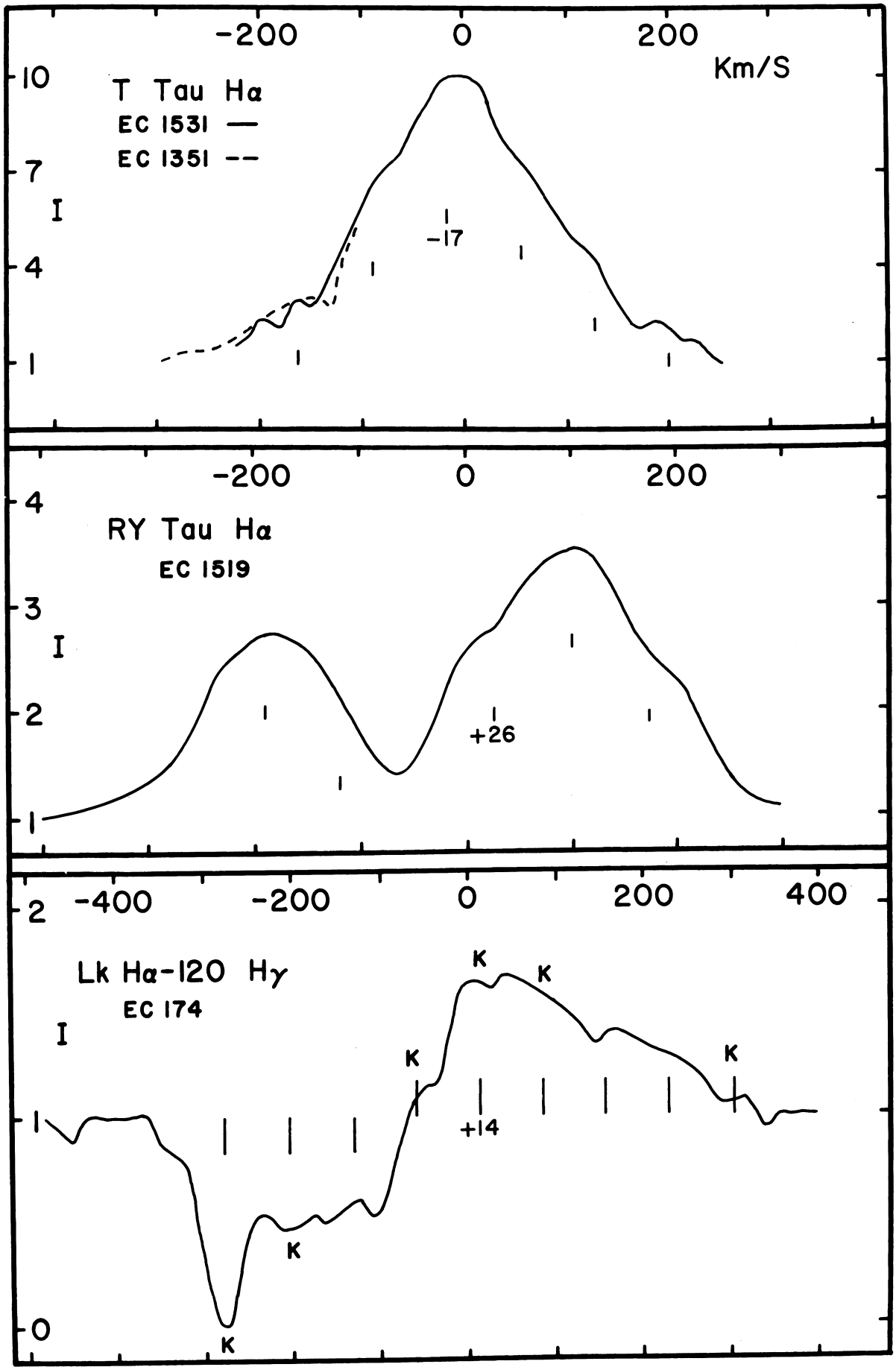
-200
0
200
Km/S
10
7
4
1
I
T Tau Hα
EC 1531 —
EC 1351 --
-17
-200
0
200
4
3
2
1
I
RY Tau Hα
EC 1519
+26
2
-400
-200
0
200
400
I
Lk Hα-120 Hγ
EC 174
K
K
K
K
K
+14
1
0

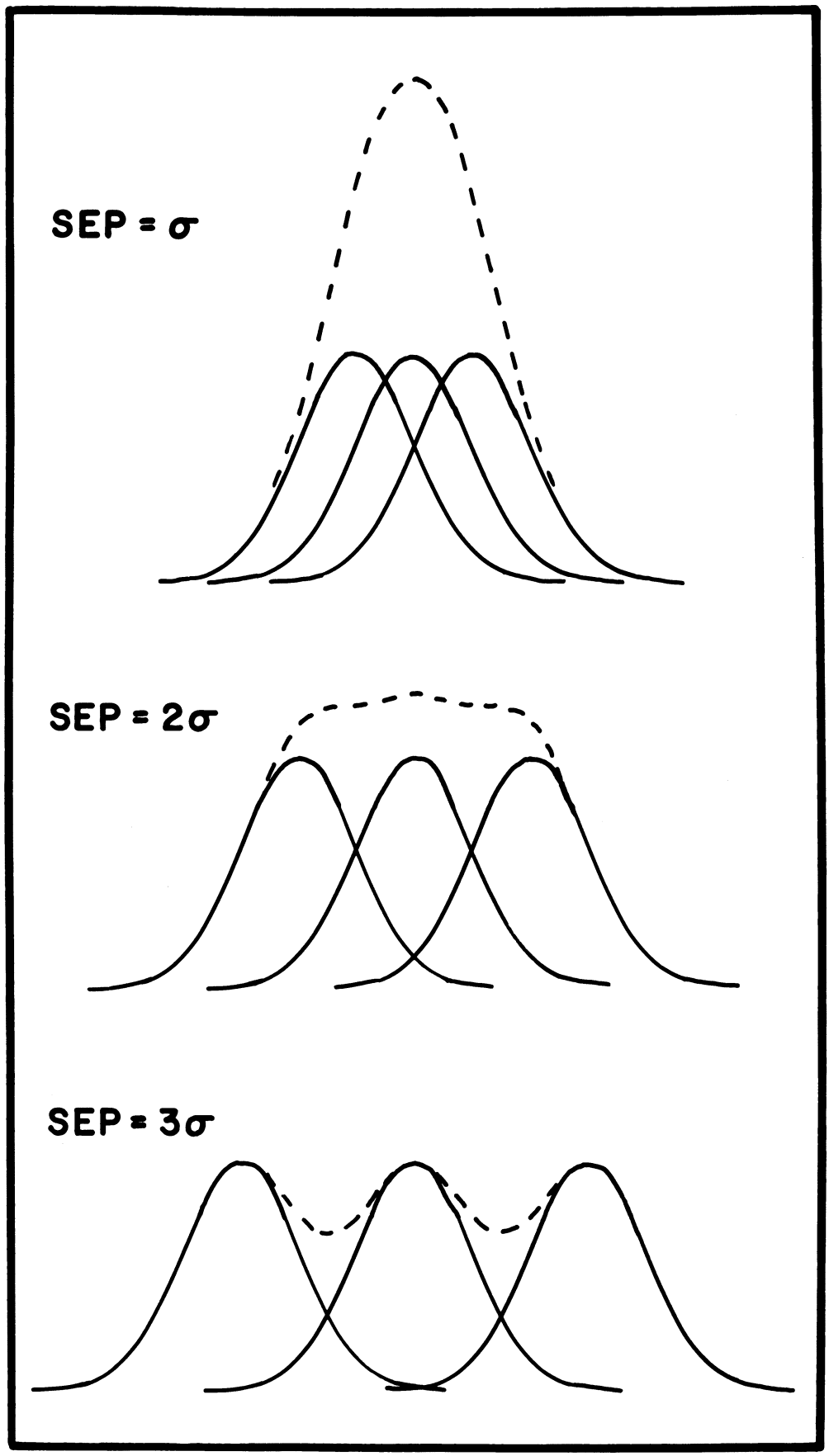
SEP = σ
SEP = 2σ
SEP = 3σ

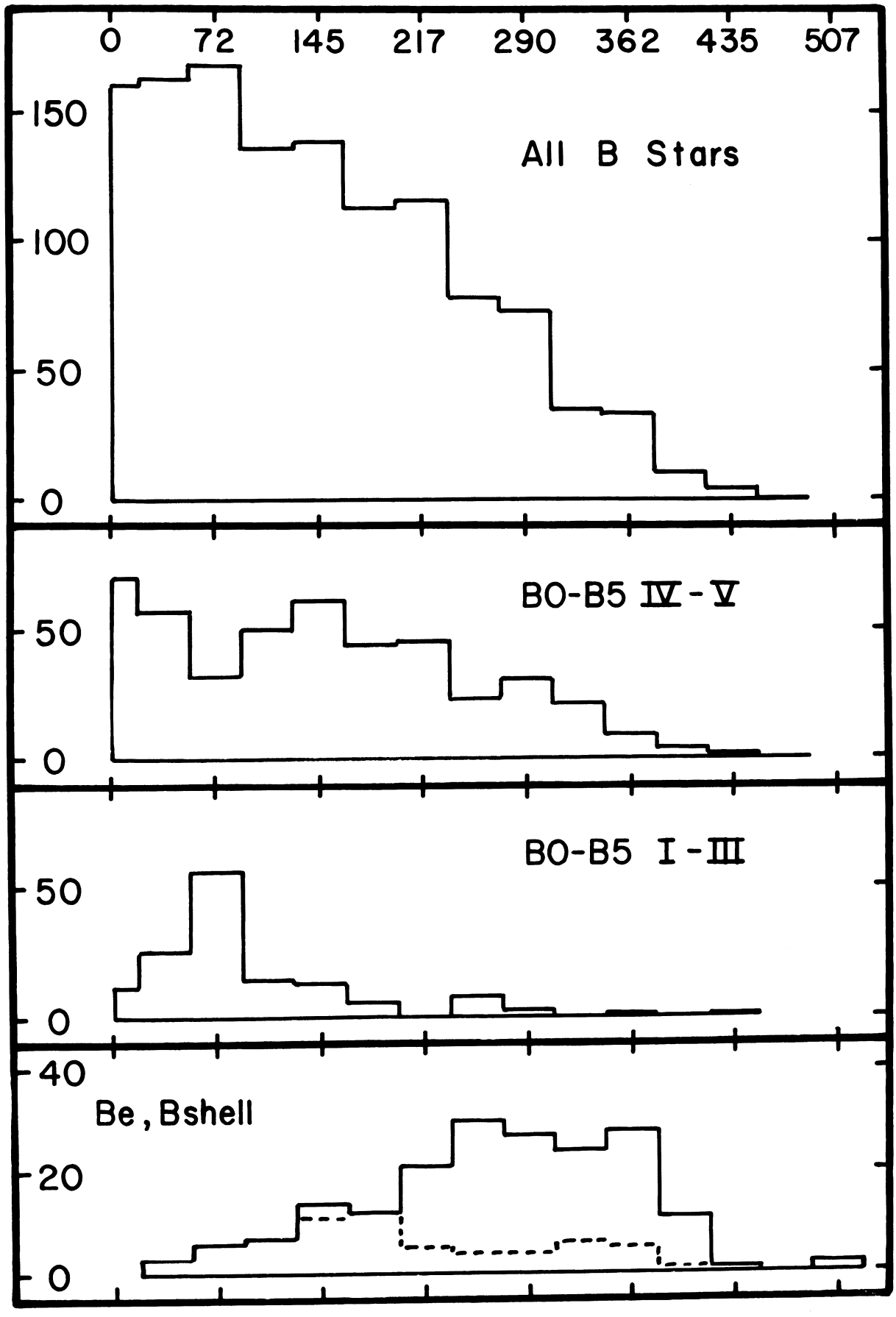
0
72
145
217
290
362
435
507
150
100
50
0
All B Stars
50
0
B0-B5 IV-V
50
0
B0-B5 I-III
40
20
0
Be, Bshell

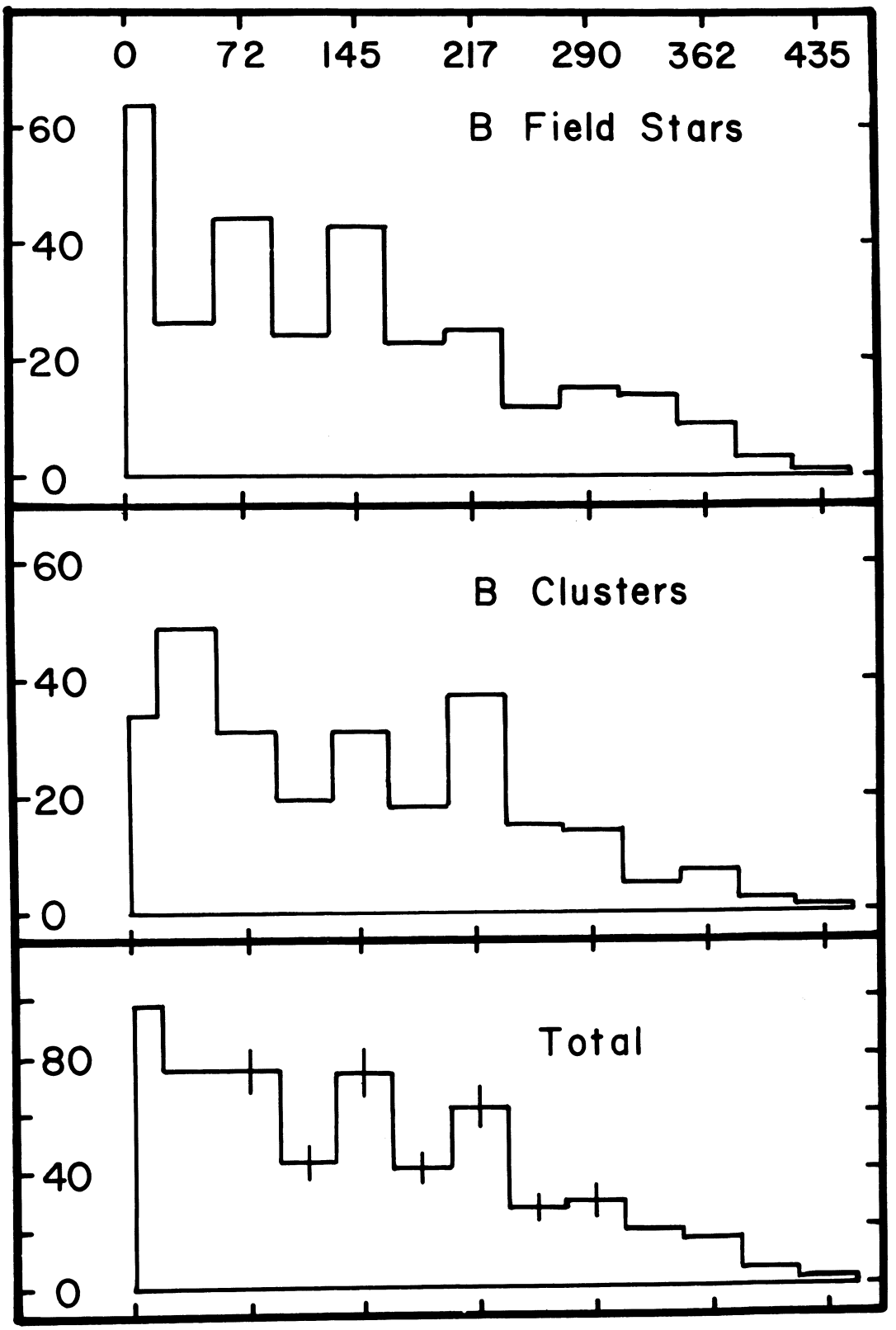
0
72
145
217
290
362
435
B Field Stars
60
40
20
0
B Clusters
60
40
20
0
Total
80
40
0

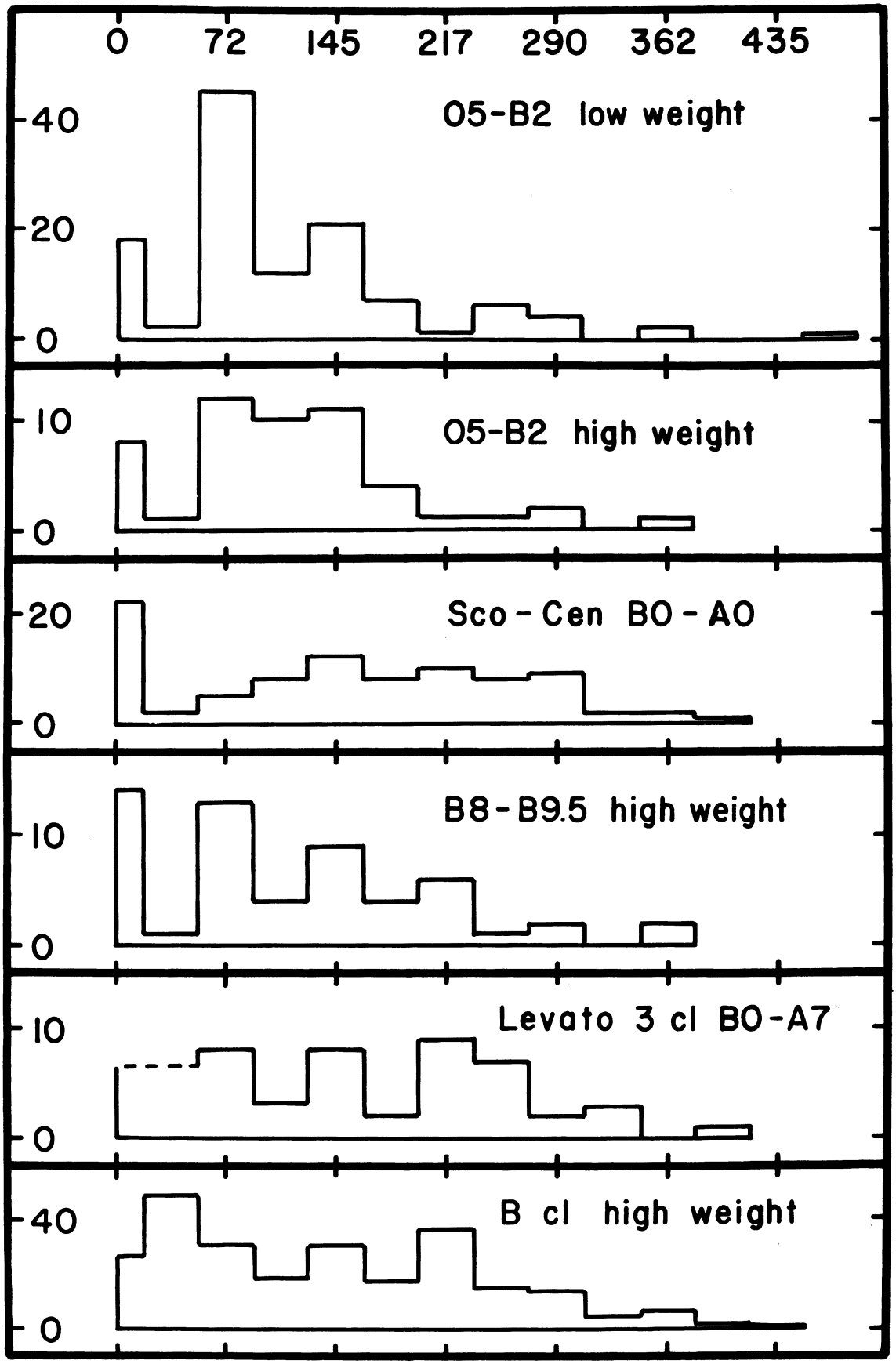
0
72
145
217
290
362
435
40
20
0
O5-B2 low weight
10
0
O5-B2 high weight
20
0
Sco - Cen BO - AO
10
0
B8 - B9.5 high weight
10
0
Levato 3 cl BO - A7
40
0
B cl high weight

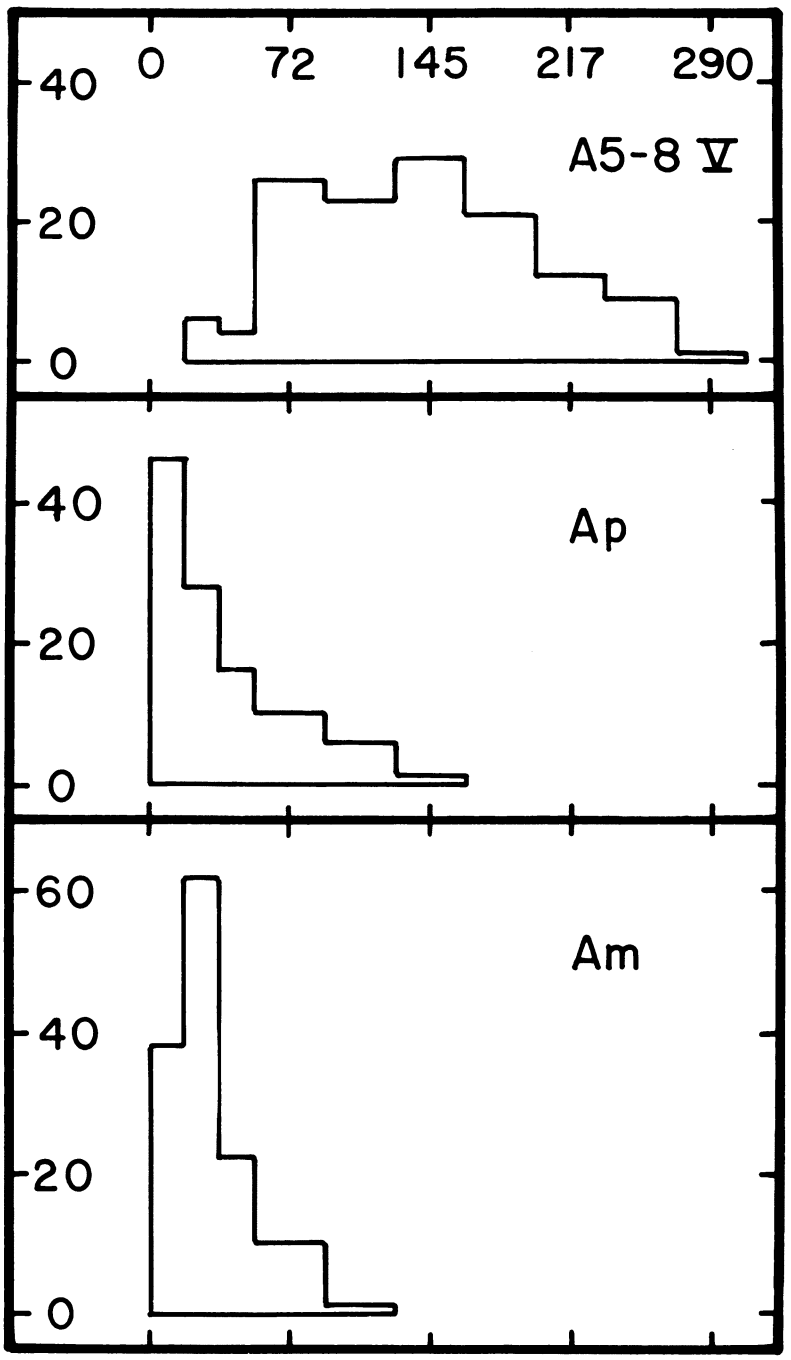
0
72
145
217
290
40
20
0
A5-8 V
40
20
0
Ap
60
40
20
0
Am

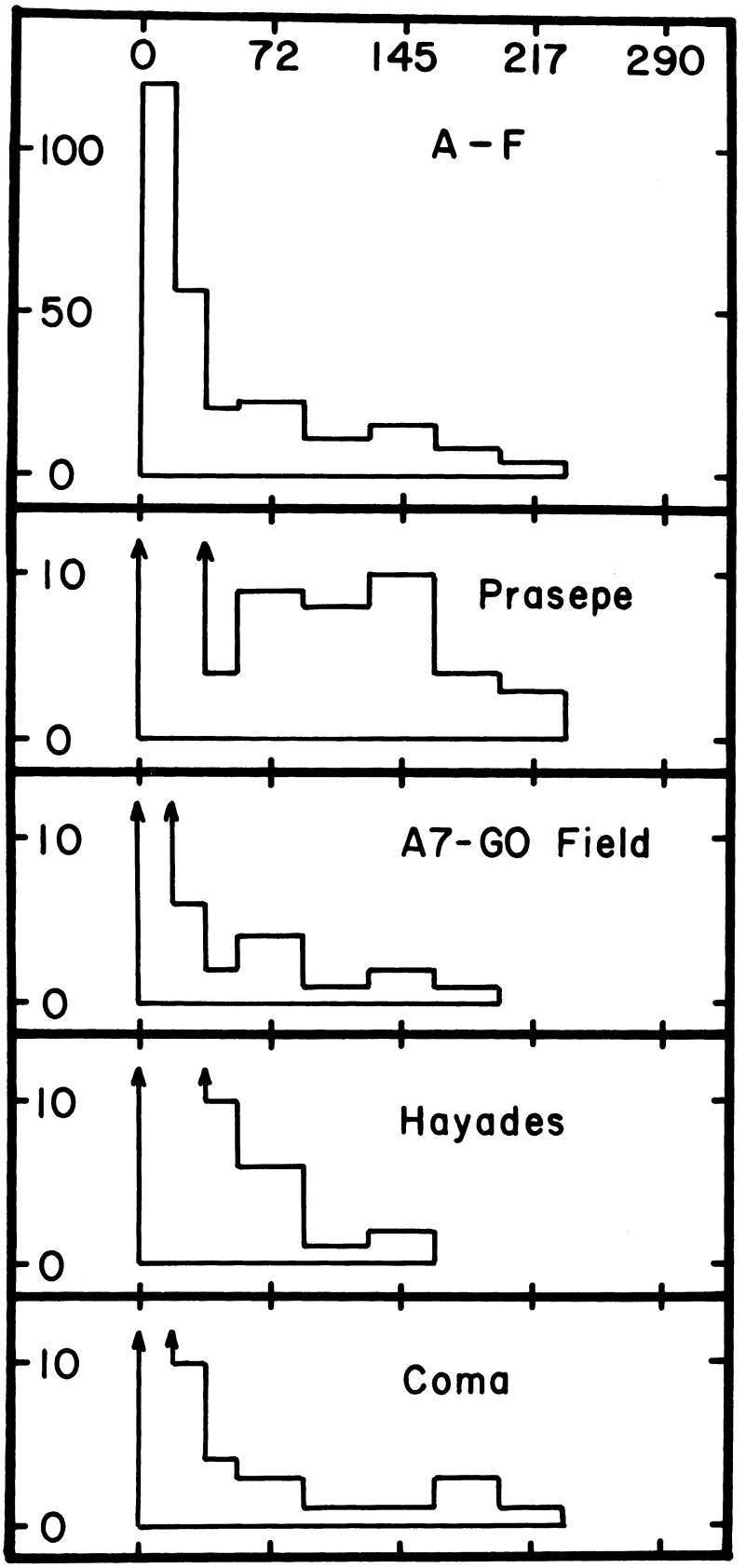
0
72
145
217
290
100
50
0
A - F
10
0
Prasepe
10
0
A7-GO Field
10
0
Hayades
10
0
Coma

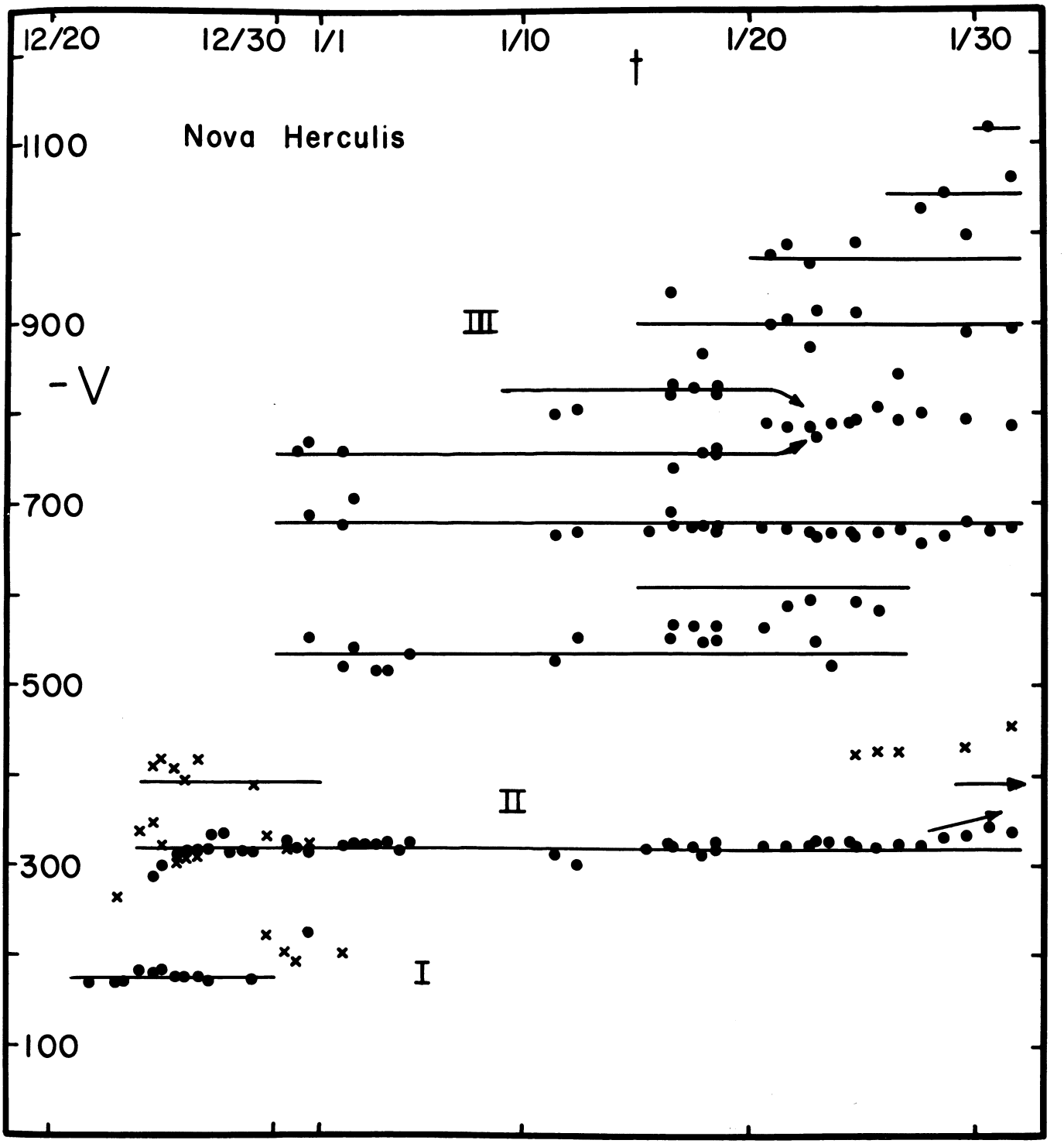
12/20
12/30
1/1
1/10
1/20
1/30
t
Nova Herculis
1100
900
700
500
300
100
-V
III
II
I

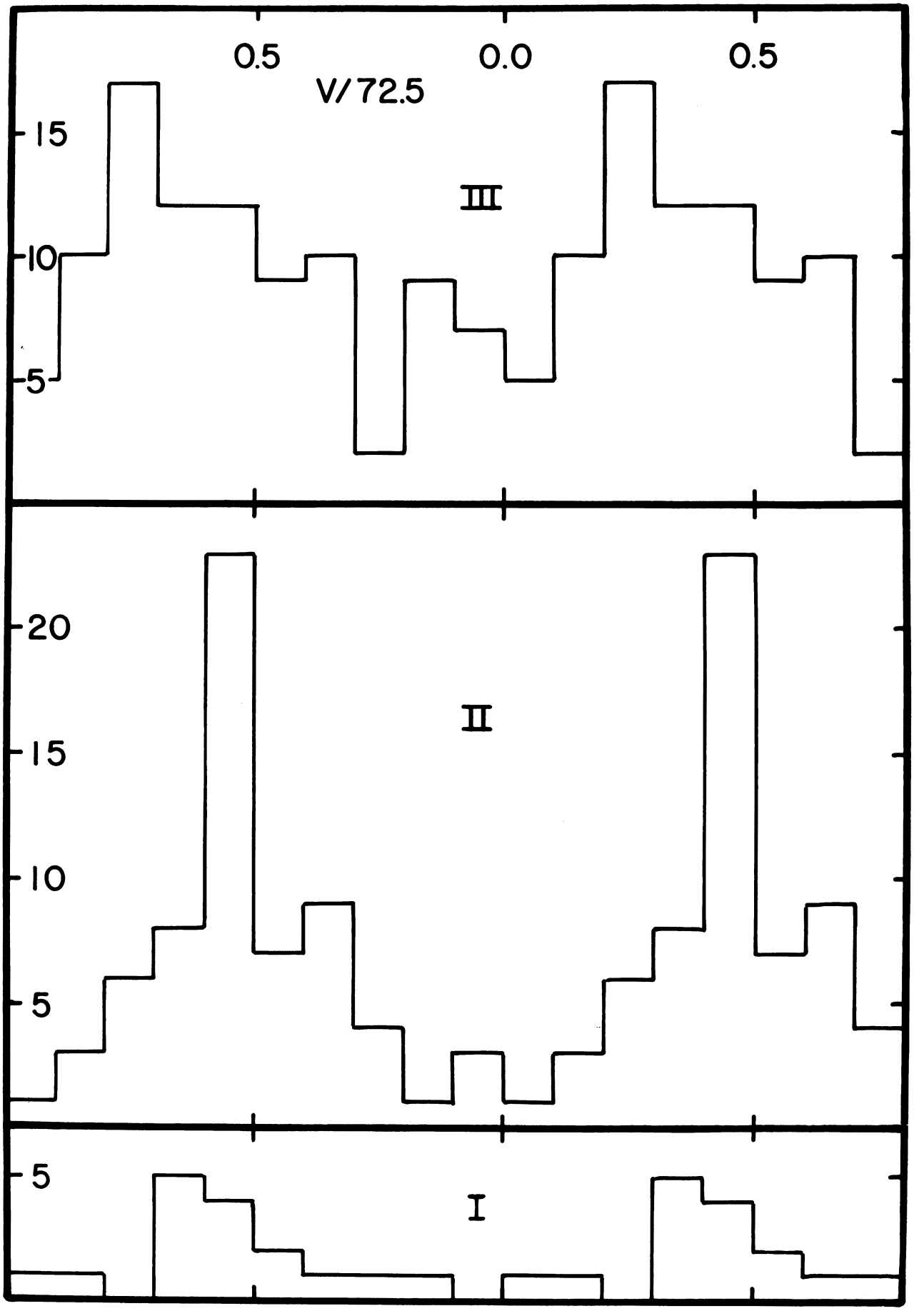
0.5
0.0
0.5
V/72.5
15
10
5
III
20
15
10
5
II
5
I